Updated Performance Comparison of a 1.5 kW Hall Thruster with Center-Mounted and Outer-Pole-Mounted Heaterless Cathodes

IEPC-2019-791

Presented at the 36th International Electric Propulsion Conference
University of Vienna, Austria
September 15-20, 2019

Thomas M. Andreano,* Davide Morfei† and John D. Williams‡
Colorado State University, Fort Collins, CO, 80523, United States

and

Casey C. Farnell§
Plasma Controls LLC, Fort Collins, CO, 80526, United States

This paper is an update to research previously published and presented at the 2019 AIAA Propulsion and Energy Forum. Heaterless, instant-start hollow cathodes using inserts made from a ceramic-metal composite (cermet) are now being used in Hall Effect thrusters at Colorado State University (CSU). Two designs of these cathodes, a 6.4 mm tubular hollow cathode and a novel planar cathode were used to study the effect of mounting location on the performance of a 1.5 kW Hall thruster. Both cathode tips were located on planes coincident with the downstream faces of the inner and outer pole pieces - with the 6.4 mm hollow cathode installed along the centerline of the inner magnetic coil, and the planar cathode installed on the upstream surface of the outer pole piece near the separatrix of the magnetic field. Performance data are presented and discussed.

Nomenclature

g_0	Standard gravitational acceleration
$I_{sp,a}$	Anode specific impulse
I_b	Beam current
I_d	Anode supply current
$\dot{m}_a$	Anode mass-flow-rate
T	Thrust
V_d	Discharge voltage
V_{avg}	Average ion voltage
η_a	Anode efficiency
η_b	Current utilization efficiency
η_v	Voltage utilization efficiency

*Graduate Research Assistant, Mechanical Engineering, thomas.andreano@colostate.edu
†Visiting Graduate Scholar, Mechanical Engineering, davide.morfei@gmail.com
‡Professor, Mechanical Engineering, drjohndarylwilliams@gmail.com
§Senior Research Engineer, casey.farnell@plasmacontrols.com

I. Introduction

Hall-Effect thrusters (HETs) make use of strong, primarily radial magnetic fields and primarily axial electric fields created within an annular channel for ionization and acceleration of a propellant. Electrons, entering the thruster from a cathode or freed from propellant atoms by ionization events, drift azimuthally around the channel due to the Hall effect caused by the crossed magnetic and electric fields in this region.[1] This movement of the electrons creates an embedded circulating current referred to as the Hall current. Propellant ions created at high positive electric potential inside or near the exit of the channel are accelerated to high exhaust velocities by the axial electric field. The cathode is a critical part of the overall operation of an HET, as it is used to produce the electrons that neutralize the ion beam expelled from the thruster and to initialize the plasma discharge in the thruster channel.[2] Hall thrusters typically utilize hollow cathodes with an integrated heating element to thermally prime a low work function insert before operation. The heating element takes the form of a resistive coil wrapped around the cathode tube that is itself nested within an enclosed keeper assembly. A dedicated power supply drives an electric current through the coil, heating the cathode until the insert begins to thermionically emit electrons and, shortly thereafter, produce a plasma discharge through the action of power supplies that bias the keeper and anode electrodes positive relative to the cathode. The cathode heater power supply is one of five used to start and operate a Hall thruster two supplies for the inner and outer electromagnets which shape the magnetic field structure, a fourth supply powers the keeper during ignition, and a fifth biases the anode to maintain the plasma discharge. Through the introduction of a heaterless hollow cathode (HHC), the cathode heater power supply can be removed enabling a simplification of the Hall thruster system. HHCs, in addition, eliminate a potential area of failure by removing the heater element that is susceptible to thermal-cycle fatigue and electro-thermal degradation over life.[3]

The mechanisms of HHC ignition are well explained in Ref.s 3 and 4. Aston conducted an early study of an HHC in 1981 using a refractory cathode tube to produce a microplasma discharge.[5] Notable in Astons cathode configuration was the omission of a low work function insert to aid in the initiation and operation of the cathode. Research was later conducted on HHCs with impregnated inserts,[4,6–8] and some studies have investigated HHCs using LaB_6 inserts as well.[9–11] Several studies, predominantly from outside the U.S., have sought insight into the effects of HHCs when used with Hall thrusters.[7,9,12–15] HHCs using versions of a barium-impregnated insert have been reported running with SPT-100 thruster,[7,12] and Loyan et al. tested an HHC at a center-mounted position and an external position near the separatrix.[14] Mounting the cathode near the separatrix has been suggested by both Hofer et al. and Sommerville et al.[16,17] In addition, Jameson et al. found a 2-3% increase in total efficiency of a Hall thruster when moving from an externally mounted cathode to an internally mounted cathode.[18]

A number of formulations for the barium-impregnated insert are used in hollow cathodes that are produced commercially through a series of complex processes, which are reflected in the high cost of these inserts. A partnership between Colorado State University and Plasma Controls, LLC, has enabled the production of barium-based, ceramic-metal composite (cermet) inserts made with an alternative, streamlined process resulting in low work function cathode inserts of comparatively lower cost. The nature of the process along with the close proximity of these partnered institutions have allowed for flexibility in the development of hollow cathodes of varying sizes and configurations with cermets of customizable compositions.[19]

This paper presents the results of experiments investigating the performance of a laboratory model SPT-100 style Hall thruster using heaterless cathodes that incorporate low work function cermets made through the streamlined process discussed previously. Two designs of the heaterless cathodes were made and installed at two positions within the Hall thruster: 1) internally center-mounted within the inner magnet core, and 2) in-plane of the outer magnetic pole, placed within the separatrix of the magnetic field topography. Thrust data were collected using a hanging double-pendulum thrust stand, and plasma plume characteristics were collected using electrostatic analyzer (ESA) and Faraday diagnostic probes. This paper also introduces the novel design of a compact, instant-start hollow cathode referred to as the postage stamp cathode, whose planar geometry makes it relatively easy to paste onto the outer pole-piece of the thruster, naturally drawing comparisons to a postage stamp being pasted onto the corner of an envelope.

II. Experimental Apparatus and Procedure

A. Laboratory Hall Thruster

The CSU Hall thruster, shown in Fig. 1a, is styled after an SPT-100 Hall thruster and operates within an input power range of 1 kW to 2 kW. The thruster was initially designed for operation at 1.5 kW and 300 V. The discharge channel is constructed from borosil (BN-SiO_2) with an outer diameter of 104 mm, a channel width of 17 mm, and a channel length of 32 mm. The thruster uses four discrete electromagnetic coils for the outer pole and a single coil for the inner pole. Magnetic shielding is not used with the current iteration of this thruster, rather a plasma lens topography with concave, symmetric field lines is utilized. The postage stamp cathode is the black disk shown on the right side of the outer pole-piece in Fig. 1a and as a 3D model in Fig. 1b.

(a)

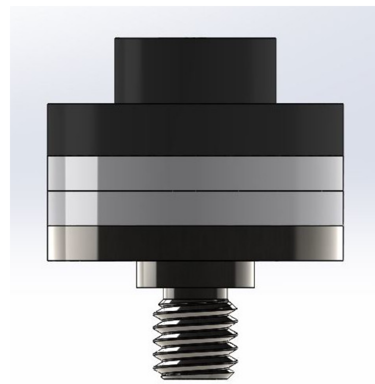

(b)

Figure 1: (a) CSU Hall Thruster with both cathodes installed. (b) Side-view of the postage stamp 3D model

B. Heaterless Hollow Cathodes

The hollow cathodes constructed for this study use low work function inserts made with a 5:3:2:0.5 formulation of BaO, CaO, Al_2O_3, and Sc_2O_3, respectively. The ceramic constituents were combined with tungsten powder in a patented process described by Farnell et. al[19] to produce the electron emitter cermet composite assembled in each cathode. A hollow cathode of traditional tubular design was made using a small-diameter, right-cylinder cermet insert installed at the downstream end of a 6.4 mm diameter Ta tube which was rolled down to form a rounded, integral orifice plate. The cathode tube orifice was roughly 1.15 mm at the time of this study. The completed cathode was rated to produce up to 10 A of electron current, and it was center-mounted inside the core of the inner magnet coil as suggested by Hofer et. al,[16] but without an enclosed keeper assembly. Rather, the keeper electrode is a disk with a 3.75 mm orifice placed over the end of the hole in the inner magnet coil as patented by Martinez et. al.[20] A second cermet was fashioned into a small disk with an approximate diameter of 9 mm and a thickness of 2.5 mm and installed in the compact postage stamp cathode. The postage stamp, as seen in Fig. 1, is nominally rated for an emission current of 7 A and has general envelope dimensions measuring 28.5 mm in diameter and 21 mm from the baseplate to the keeper orifice. The keeper orifice diameter was roughly 2.15 mm at the time of this study. When installed in the thruster, the downstream surface of the keeper for the postage stamp was positioned to be coincident with the plane of the outer pole piece with the keeper orifice located within the separatrix of the magnetic field structure as first demonstrated by Murashko et al.[15]

C. Facility, Power Supplies, Propellant Delivery, Thrust Stand, and Plasma Diagnostics

A vacuum chamber measuring 1.7 m in diameter and 4.6 m in length was used for all tests. The chamber is equipped with a Leybold DryVac roughing pump, two Varian HS20 diffusion pumps, and two internal cryosails, the layout of which is shown in Fig. 2. The chamber is capable of reaching a base pressure of 9.0

x 10^{-7} Torr with a maximum pumping speed of 38,000 L/s on krypton. A graphite beam dump, located 2.8 m downstream of the thrust stand, separates the cryosails from direct exposure to the thruster plume.

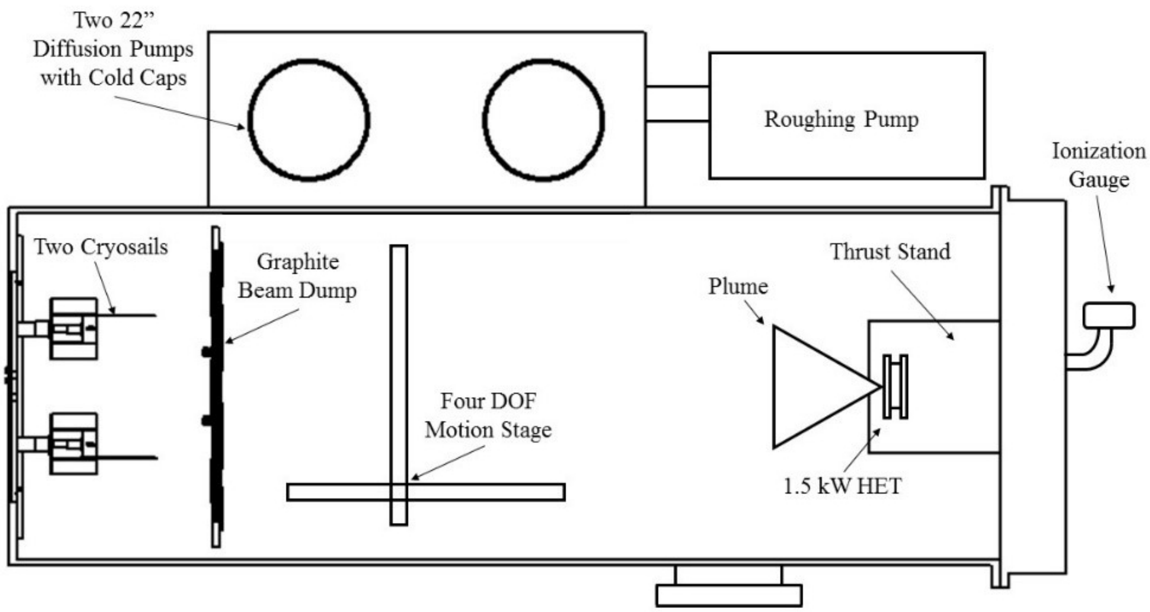

Figure 2: Schematic of the vacuum chamber used in this study.

Four laboratory power supplies, with the notable absence of a cathode heater supply, are used to operate the HET. Both cathodes were installed so as to be electrically connected outside of the test chamber. A 2.2 ohm resistor was placed between the anode and discharge power supply, and two 100 ohm resisters in parallel were placed between the keeper and the keeper supply to avoid excessive current flow at start-up. Two oil tank capacitors each rated at 54 F were wired in parallel to each other and placed in parallel with the anode and cathode downstream of the anode ballast resistor to filter the anode power supply from plasma oscillations. Blocking and freewheeling diodes were also included in the circuit to protect the keeper and anode power supplies from unstable operation. High-purity krypton gas (99.999%) was delivered to the cathodes and anode through three dedicated, stainless steel gas lines and controlled by 50 and 100 sccm mass flow controllers (used for the cathode and anode, respectively).

Thrust measurements were captured using a hanging double pendulum thrust stand. The stand uses a linear-variable-differential transformer (LVDT) in combination with an SRS lock-in amplifier to measure the displacement of the stand. Calibration of the stand is achieved by applying known forces to the stand via hanging weights and recording the voltage produced by the LVDT to create an equation relating the voltage measured by the LVDT and the applied force. The calibration is repeated when the system has reached thermal equilibrium to account for transient thermal effects.

During testing, an electrostatic analyzer (ESA) and a Faraday probe were used to measure the energy and current density, respectively, of ions in the plume. The ESA sits stationary on a platform 2 meters downstream from the face of the thruster, and the Faraday probe is mounted on a motion stage with four degrees of freedom. A Keithley 6517A was used to provide a voltage sweep to the ESA. The transmission energy of the ESA was set to 400 eV. The Faraday probe was biased at -20 V relative to the cathode.

D. Test Procedure

Prior to testing, the diffusion and cryo pumps were allowed to pump on the vacuum chamber overnight, so as to bring the background pressure of the chamber into the 10^{-7} Torr range. Specifically, the center-mounted cathode was run with a background pressure of 9.70×10^{-7} Torr, and the postage stamp cathode was run with a background pressure of 9.42×10^{-7} Torr. Chamber pressure during operation ranged from 5.72×10^{-5} to 6.91×10^{-5} Torr with the center-mount cathode, and from 6.13×10^{-5} to 7.63×10^{-5} Torr with the postage stamp cathode. After initial start-up of the HET, it was allowed to warm up for two hours to ensure nominal, repeatable operation. The thrust stand was calibrated after the warm-up period with the thruster on, at an anode mass-flow-rate of 4.5 mg/s. After calibration, the discharge voltage and the krypton flow-rates were then set to each of the tested set-points. The cathode was run at a constant .346 mg/s (5.55 sccm) for every set-point, chosen because it is less than 10% of all of the anode flows studied, and was the lowest cathode flow-rate that provided steady operation with the center-mounted cathode. With the flow-rates and discharge voltage set, the currents supplied to the inner and outer coils were adjusted until the discharge current was minimized. Once this optimized operating condition was found, the ESA and Faraday probe data were taken and all supplied voltages, currents, and flow rates were recorded. Next, a thrust measurement was taken by shutting off the thruster to provide a differential thrust measurement. The average of 100 "zero" measurements was subtracted from the average of 100 "thrusting" measurements to obtain the actual thrust force. One set of data was collected with each cathode configuration in April 2019, and a second set of data was collected with the postage stamp cathode configuration in September 2019 using a new keeper.

E. Performance Metrics

The performance calculations were made using the thrust measurement and the recorded input flows, voltages, and currents. As is conventional with laboratory Hall thrusters, the performance metrics considered were anode specific impulse and anode efficiency, due to the probability of imperfectly optimized magnetic circuits and/or cathode operation. Equations 1 and 2 were used to calculate these metrics.

$$I_{sp,a} = \frac{T}{\dot{m}_a g_0} \tag{1}$$

$$\eta_a = \frac{T^2}{2 V_d I_d \dot{m}_a} \tag{2}$$

In addition, the data from the ESA probe were used to calculate voltage utilization efficiency, shown by Eq. 3. Equation 4 is used to calculate current utilization efficiency using the beam current, integrated from Faraday probe data.

$$\eta_v = \frac{V_{avg}}{V_d} \tag{3}$$

$$\eta_b = \frac{I_b}{I_d} \tag{4}$$

III. Results and Discussion

Figure 3 contains plots of thrust as a function of discharge voltage, which was varied from 250 V to 350 V, at each anode flow-rate, which was varied from 4.25 to 5.25 mg/s (krypton). The thrust produced by the CSU Hall thruster fell between 59.6 and 85.0 ± 1.5 mN with the center-mount cathode, between 57.0 and 85.4 ± 1.5 mN in the first set of data with the postage stamp cathode, and between 58.6 and 87.8 ± 1.5 mN in the second set of data with the postage stamp cathode. The thrust increased with discharge voltage at each anode flow condition, as expected. During the initial testing, center-mount cathode configuration produced higher thrust in all cases except for the conditions [325 V, 4.75 mg/s], [325 V, 5.0 mg/s], and [325 V, 5.25 mg/s]. At all operating conditions except those three, the postage stamp cathode configuration was shown to result in 1-3 mN lower thrust compared to the center-mounted configuration. We note that the estimated error in the thrust measurements is ± 1.5 mN which is close to the difference between the two cathode configurations at many of the operating points. During the second round of testing with the postage stamp cathode, thrust was typically higher by 1-5 mN than that produced with either configuration during initial testing. This may be a result of better alignment of the magnetic coils and thruster channel.

The anode efficiency of the thruster ranged from 30.8% to 36.4% with the center-mount cathode, from 27.9% to 37.2% in the initial testing with the postage stamp cathode, and from 30.2% to 35.6% in the second set of data with the postage stamp cathode. Plots of the anode efficiency as a function of discharge voltage, contained in Fig. 4, show a general trend of 0.5-3% lower efficiency for the postage stamp cathode during initial testing, however, the postage stamp had higher efficiency at five of the eighteen operating conditions: [4.5 mg/s, 325 V], [4.75 mg/s, 325 V], [5.0 mg/s, 325 V], [5.25 mg/s, 250 V], and [5.25 mg/s, 325 V]. Although these data points suggest a possible advantageous discharge voltage for the postage stamp cathode at 325 V, we point out that this result could also be explained by non-ideal optimization of the electromagnets during the center-mounted cathode testing at that operational set-point and by uncertainty in the anode efficiency values that is roughly estimated to be ± 3%. During the second set of testing with the postage stamp configuration, anode efficiency was generally near the values of the initial testing. In comparison, a flight model SPT-100 running on krypton propellant was shown by Nakles et al.[21] to have anode efficiency ranging from roughly 32% to 45% for discharge voltage varying from 250 V to 350 V and anode flow varying from 4.09 mg/s to 5.31 mg/s.

As expected, the anode specific impulse data, contained in Fig. 5, show a similar trend to the thrust data in Fig. 3. The center-mount configuration produced anode I_{sp} ranging from 1430 seconds to 1684 seconds. The postage stamp configuration produced anode I_{sp} ranging from 1368 seconds to 1658 seconds during initial testing, and from 1407 seconds to 1706 seconds during the second round of testing. In addition, similar to thrust, the anode I_{sp} increased with increasing discharge voltage.

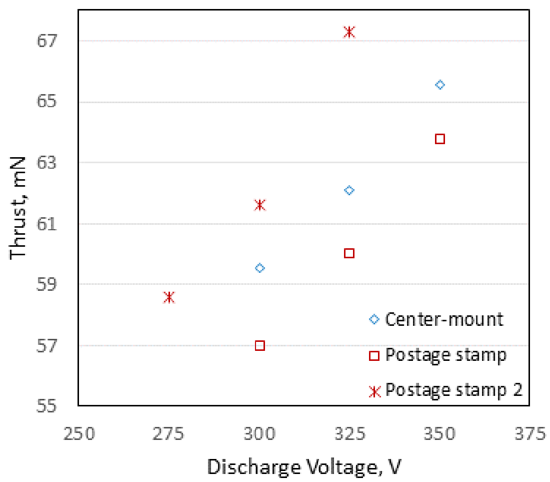

(a) 4.25 mg/s krypton

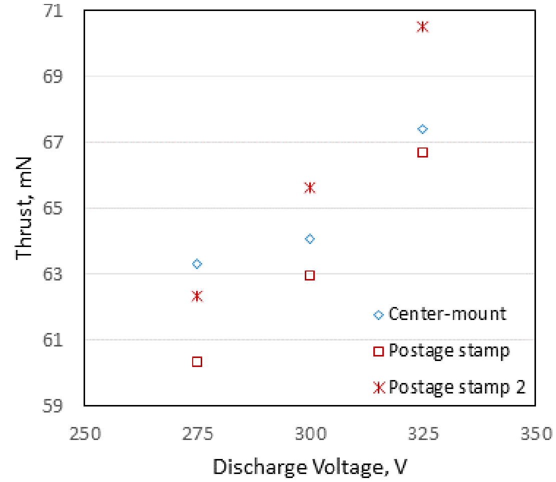

(b) 4.5 mg/s krypton

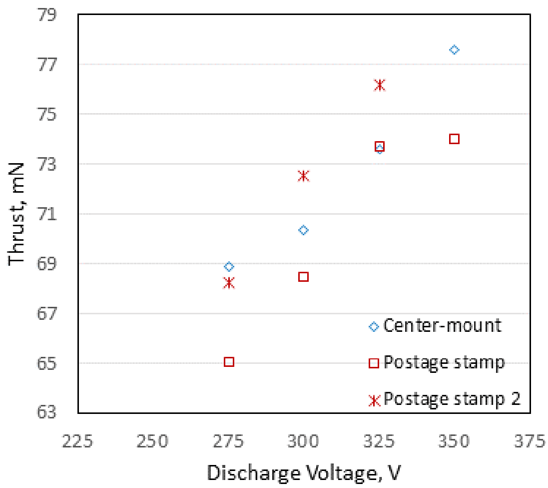

(c) 4.75 mg/s krypton

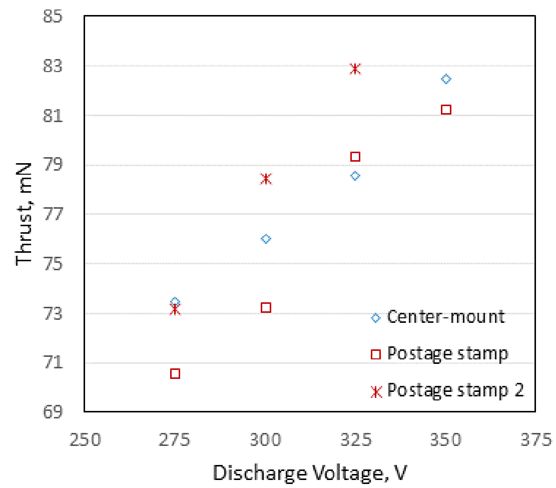

(d) 5.0 mg/s krypton

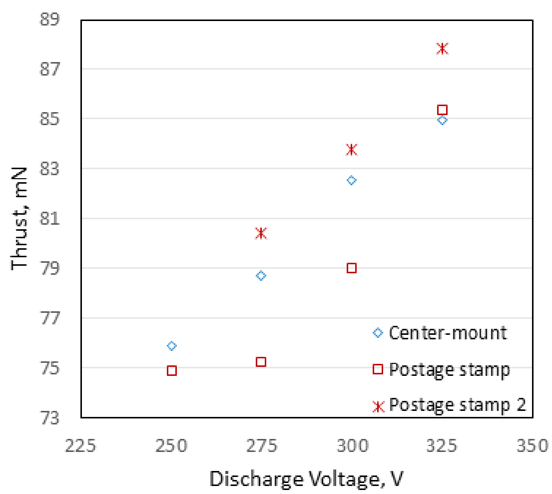

(e) 5.25 mg/s krypton

Figure 3: Thrust as a function of discharge voltage and anode mass flow-rate

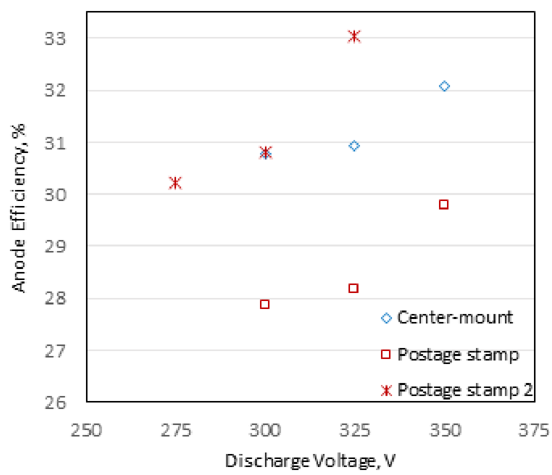

(a) 4.25 mg/s krypton

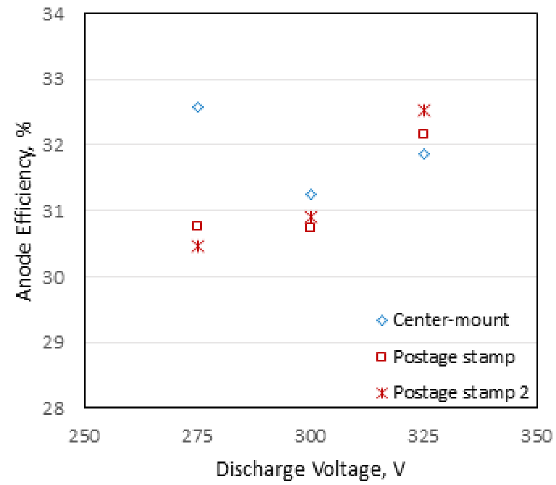

(b) 4.5 mg/s krypton

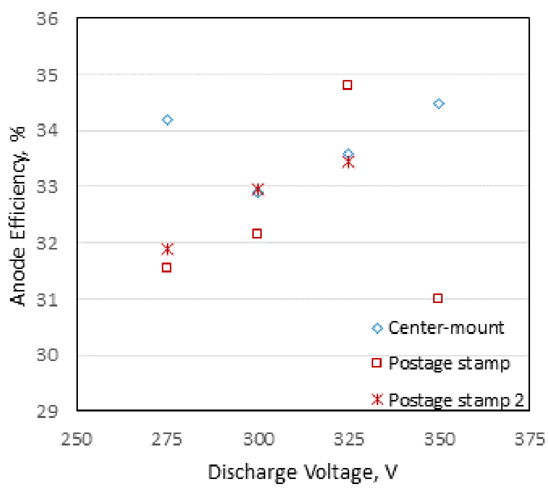

(c) 4.75 mg/s krypton

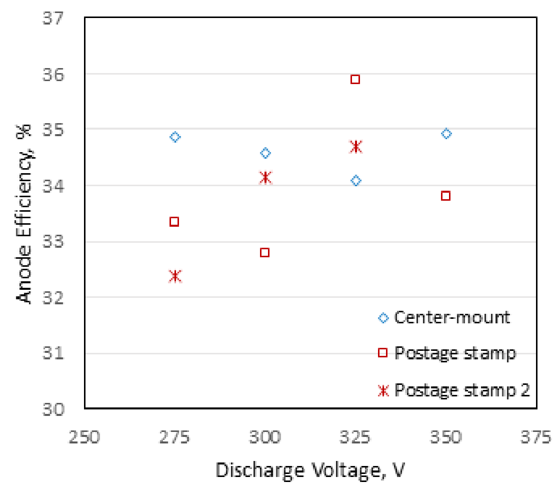

(d) 5.0 mg/s krypton

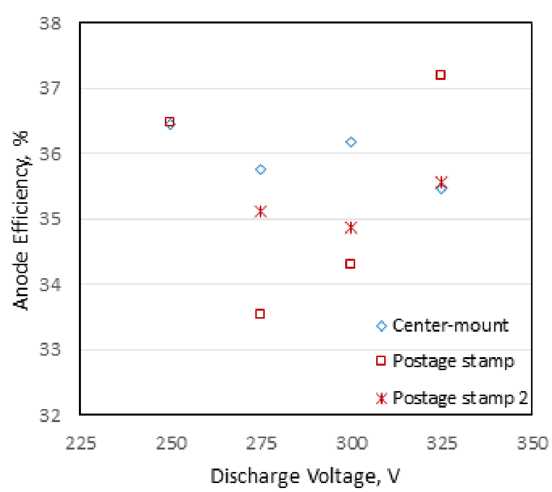

(e) 5.25 mg/s krypton

Figure 4: Anode efficiency as a function of discharge voltage and anode mass flow-rate

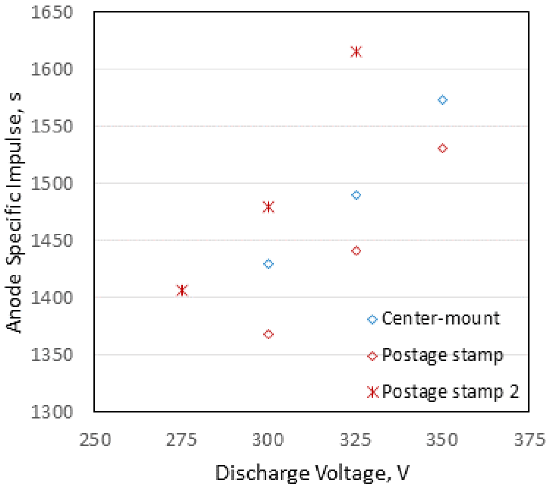

(a) 4.25 mg/s krypton

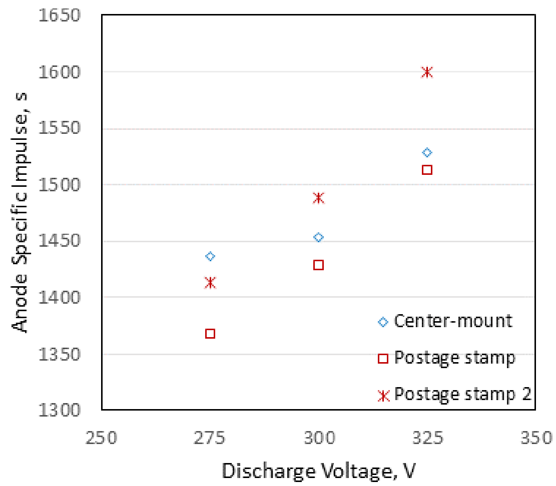

(b) 4.5 mg/s krypton

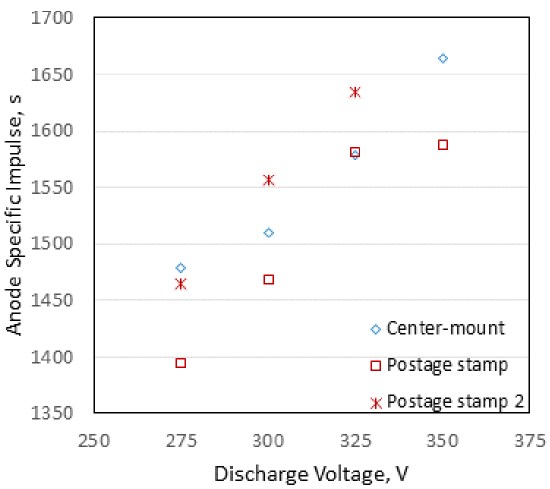

(c) 4.75 mg/s krypton

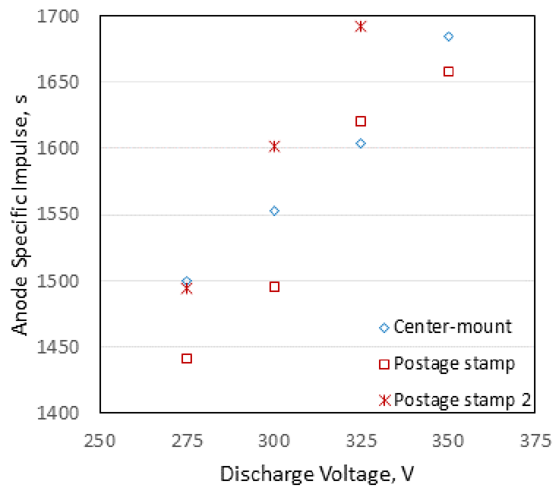

(d) 5.0 mg/s krypton

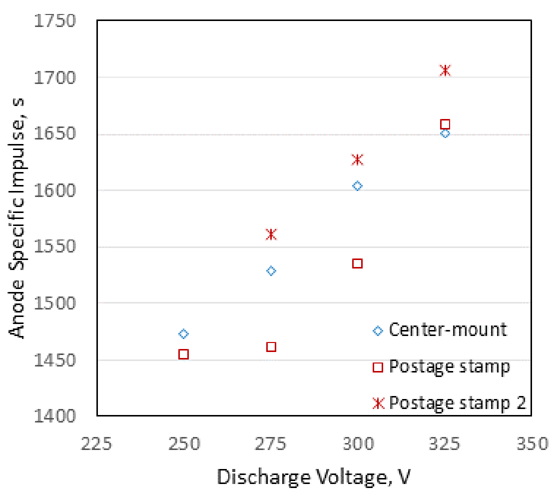

(e) 5.25 mg/s krypton

Figure 5: Anode specific impulse as a function of discharge voltage and anode mass flow-rate

ESA data were only analyzed for the initial testing of the two configurations. In contrast to the performance data contained in Figs. 3 - 5, the voltage utilization efficiency, plotted in Fig. 6, was actually higher for the postage stamp configuration compared with the center-mounted cathode. This result occurs because the postage stamp exhibits a "high energy shoulder" feature in ESA traces with ions at energies higher than the discharge voltage. The presence of this feature increases the average ion energy, leading to a higher voltage utilization efficiency. Typical ESA traces comparing the postage stamp ion energy distribution function (IEDF) to the center-mount IEDF are shown in Fig. 7, which showcases this result. Interestingly, the voltage efficiency is observed to dip to a minimum at 300 V similar to the trend observed in anode efficiency. The center-mount cathode configuration resulted in a voltage utilization efficiency range from 92.3% to 95.8%, and the postage stamp cathode configuration ranged from 95.2% to 98.8%. The postage stamp cathode also had a significantly smaller spread in voltage efficiency at discharge voltages of 275 V, 300 V, and 325 V. It is also noted that while the postage stamp produced higher average ion energy because of this shoulder, the most probable energy (i.e. the peak of the function) is lower than that of the center-mount IEDF by roughly 5 eV. The Full-Width-at-Half-Max (FWHM) of the two IEDFs are within 1.5 eV of each other, the center-mount FWHM being 25.3 eV and the postage stamp FWHM being 26.8 eV. The average FWHM for all cases with the center-mount configuration was 27.1 eV with a standard deviation of 1.28 eV, and the average FWHM with the postage stamp configuration was 27.7 eV with a standard deviation of 1.60 eV. The cause of the high energy shoulder is yet unknown, but we note that the keeper orifice diameter of the postage stamp was relatively large, which might have caused the postage stamp to operate closer to the spot-to-plume mode transition than desired, where high energy ions have been shown to be produced[22].

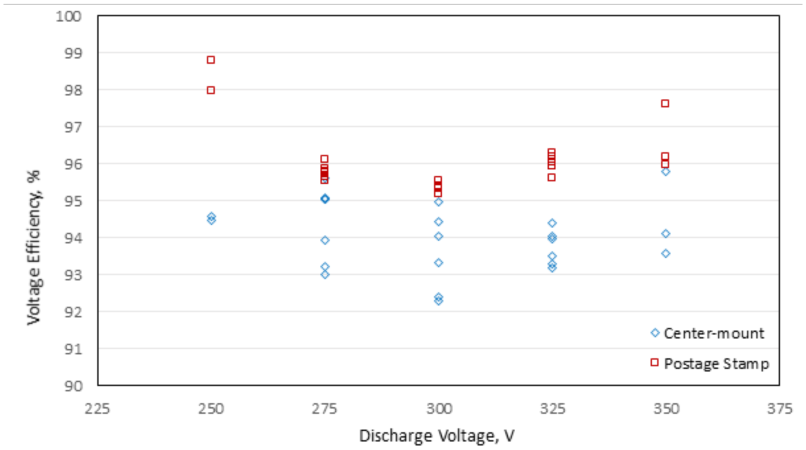

Figure 6: Voltage efficiency as a function of discharge voltage

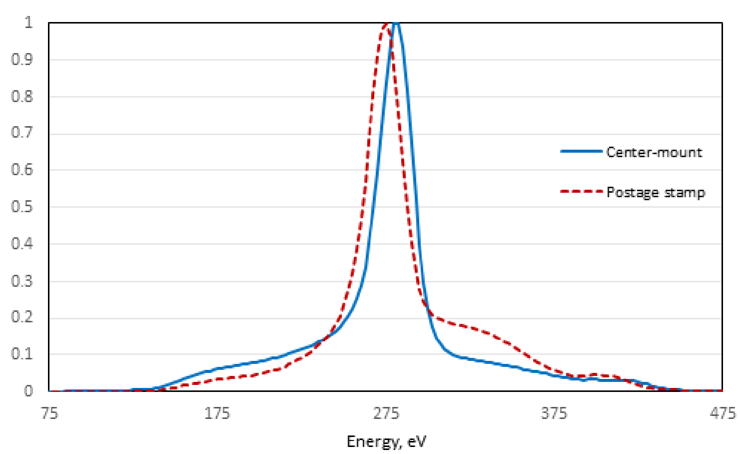

Figure 7: Normalized ESA traces at 300 V discharge voltage and 4.5 mg/s anode flow

Faraday probe current density traces were taken at a radius of 40 cm from the centerpoint of the thruster face, an example of which is shown in Fig. 8. Faraday probe data was only collected during the initial testing of the two configurations. These data will be retaken and presented in future work with further analysis because the motion stage available at the time of this study was only capable of ± 25 degrees relative to the thruster center. We note the apparent shift from the centerline and the higher peak current density of the postage stamp. This shift is most likely due to an imperfect alignment of the motion stage to the thruster centerline, but might also be explained by issues associated with repelling electrons from the Faraday probe collector when it is in the dense, energetic plasma present near the center of the thruster plume. To improve the usefulness of Faraday probe data, a new motion stage has been built to allow a larger arc to be traversed by the probe, and our beam current utilization analysis scripts are being improved along with our techniques for determining the corrected current density data using gridded ion beam sources for calibration. Although these improvements were not ready during the present study, some preliminary analysis of the Faraday probe data was performed. At this operating point, the center-mount configuration had a discharge current of 4.88 A, and the postage stamp configuration had a discharge current of 4.79 A. The integrated ion beam current was calculated to be 3.51 A with 4.0% estimated error for the center-mount configuration and 3.90 A with 6.1% estimated error for the postage stamp configuration. This results in a current utilization efficiency of 72.0% for the center-mount, and 81.4% for the postage stamp. With a higher current utilization and voltage utilization efficiency, the cause of the generally lower total efficiency for the postage stamp would have to be lower mass utilization and/or charge utilization. These metrics were not calculated for this study because our charge state probe and new motion stage (with improved beam current analysis) were not available, however, we plan to include these measurements and analysis in future work.

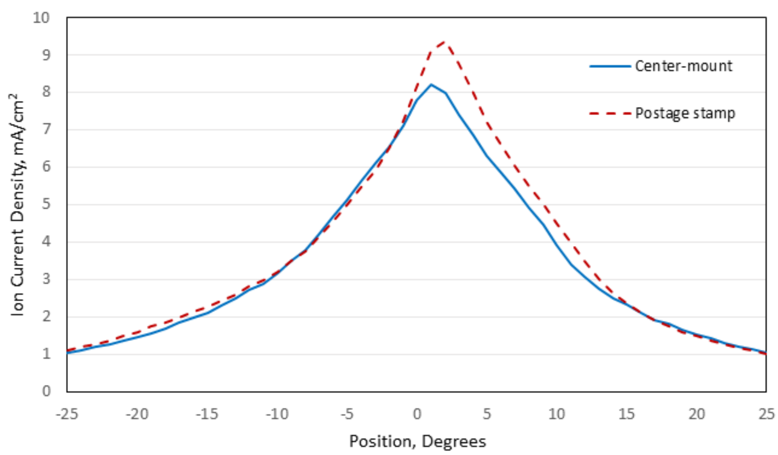

Figure 8: Faraday probe data for both cathode configurations at 300 V discharge voltage and 4.5 mg/s anode flow

In addition, data were collected with an ExB probe for the second round of testing with the postage stamp cathode. At this time, only preliminary analysis has been completed on these data. A typical trace taken with the ExB probe is shown in Fig. 9, with the y-axis normalized. This trace was taken with the thruster running at 325V discharge and 4.5 mg/s mass flow to the anode, in the postage stamp cathode configuration. The peaks for the singly, doubly, and triply charged ions are found at 30V, 41.3V, and 51.6V, respectively. These values are close to what would be expected.

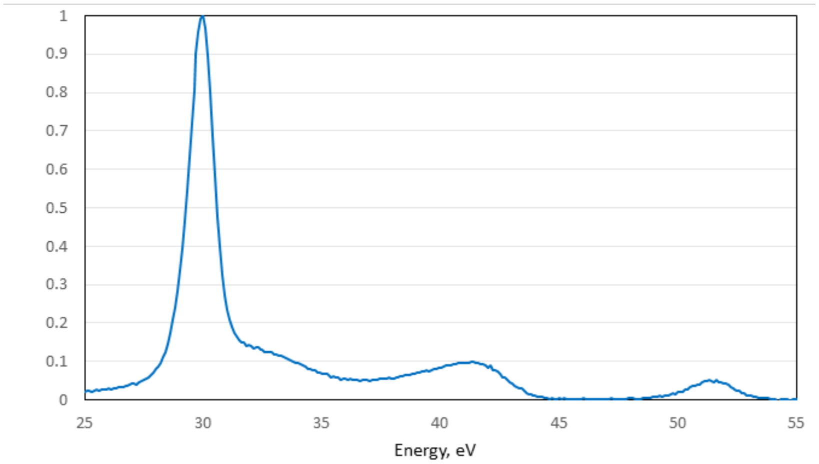

Figure 9: Normalized ExB probe trace for the postage stamp configuration at 325 V discharge voltage and 4.5 mg/s anode flow

IV. Conclusion and Future Work

A study of the Hall thruster performance differences caused by using a center-mounted cathode and an outer-pole-piece mounted cathode (the postage stamp) was conducted. Initially, it was found that performance suffers with the pole-piece mounted cathode, but the loss is small and typically falls close to or within the error of the measured values. However, a second set of data collection using the postage stamp resulted in mostly higher performance than with either of the configurations during the initial test. More investigation will have to be done, and a second set of data must be taken with the center mounted cathode to determine if there truly is any significant performance difference. When considering the potential benefits of this new cathode geometry and mounting location, such as ease of integration, it may be worth a potential small loss in overall thruster performance in certain applications. For example, a postage-stamp-style cathode could ease the scaling of Hall Effect thrusters to higher power levels by allowing multiple cathodes to be placed on the pole pieces of nested Hall thrusters rather than utilizing one large, high-current-capable, center-mounted cathode.

The 1.5 kW Hall thruster at CSU will continue to be characterized through additional testing with an ExB probe, Faraday probe, and a Hall current tomography sensor previously developed at CSU which could provide interesting insight into thruster operation at different conditions. The center-mount cathode used in the initial study has since been entirely replaced, and the authors plan to repeat the tests, varying the keeper orifice diameter for both cathodes to determine any performance differences. In addition, a new motion stage built in the time since this study will allow a larger range of motion for the Faraday probe, allowing collection of better beam current density data to be analyzed and presented in the future. Finally, more analysis of the ExB probe data will be executed to collect charge state information, allowing the determination of charge and mass utilization efficiency.

References

[1]Goebel, D., and Katz, I., *Fundamentals of Electric Propulsion*, Jet Propulsion Laboratory Space Science and Technology Series, NASA Jet Propulsion Laboratory, 2008, Chap. 7, pp. 325-330.

[2]Sommerville, J., and King, L., "Effect of Cathode Position on Hall-Effect Thruster Performance and

Cathode Coupling Voltage," *43rd AIAA/ASME/SAE/ASEE Joint Propulsion Conference & Exhibit*, AIAA 2007-5174, Cincinnati, OH, 2007.

[3]Lev, D., and Appel, L., "Heaterless Hollow Cathode Technology - A Critical Review," *Space Propulsion 2016*, SP2016_3125366, Rome, Italy, 2016.

[4]Schatz, M., "Heaterless Ignition of Inert Gas Ion Thruster Hollow Cathodes," *AIAA/DGLR/JSASS 18th International Electric Propulsion Conference*, AIAA-85-2008, Alexandria, VA, 1985.

[5]Aston, G., "Hollow cathode startup using a microplasma discharge," *Review of Scientific Instruments*, Vol. 52, 1981, pp. 1259-1260.

[6]Vekselman, V., Krasik, Y. E., Gleizer, S., Gurovich, V. T., Warshavsky, A., and Rabinovich, L., "Characterization of a Heaterless Hollow Cathode," *Journal of Propulsion and Power*, Vol. 29, No. 2, 2013.

[7]Arkhipov, B., "Development and Research of Heaterless Cathode-Neutralizer for Linear Hall Thrusters (LHD) and Plasma Ion Thrusters (PIT)," *25th international Electric Propulsion Conference*, IEPC-97-175, Cleveland, OH, 1997.

[8]Lev, D., Alon, G., Appel, L., Seeman, O., and Hadas, Y., "Low Current Heaterless Hollow Cathode Development Overview," *35th International Electric Propulsion Conference*, IEPC-2017-244, Atlanta, GA, 2017.

[9]Albertoni, R., Andrenucci, M., Pedrini, D., and Paganucci, F., "Preliminary Characterization of a LaB_6 Hollow Cathode for Low-Power Hall Effect Thrusters," *33rd International Electric Propulsion Conference*, IEPC-2013-137, Washington, D.C.,2013.

[10]Pedrini, D., Albertoni, R., Paganucci, F., and Andrenucci, M., "Development of a LaB_6 Cathode for High-Power Hall Thrusters," *Joint Conference of 30th International Symposium on Space Technology and Science, 34th International Electric Propulsion Conference, and 6th Nano-satellite Symposium*, IEPC-2015-47/ISTS-2015-b-47, Hyogo-Kobe, Japan, 2015.

[11]Daykin-Iliopoulos, A., Gabriel, S., Golosnoy, I., Kubota, K., and Funaki, I., "Investigation of Heaterless Hollow Cathode Breakdown," *Joint Conference of 30th International Symposium on Space Technology and Science, 34th International Electric Propulsion Conference, and 6th Nano-satellite Symposium*, IEPC-2015-193, Hyogo-Kobe, Japan, 2015.

[12]Albarede, L., Lago, V., Lasgorceix, P., Dudeck, M., Burgova, A., and Malik, K., "Interaction of a Hollow Cathode Stream with a Hall Thruster," *28th International Electric Propulsion Conference*, IEPC-2003-333, Toulouse, France, 2003.

[13]Koshalev, N., and Loyan, A., "Investigation of Hollow Cathode for Low Power Hall Effect Thruster," *30th International Electric Propulsion Conference*, IEPC-2007-103, Florence, Italy, 2007.

[14]Loyan, A., Titov, M., Rybalov, O., and Maksymenko, T., "Middle power Hall Effect Thrusters with centrally located cathode," *33rd International Electric Propulsion Conference*, IEPC-2013-410, Washington, D.C., 2013.

[15]Murashko, V., Koryakin, A., Nesterenko, A., Olotin, S., Oranskiy, A., Loyan, A., Koshelev, M., Bilokon, V., and Nesterenko, S., "Russian Flight Hall Thrusters SPT-70 & SPT-100 After Cathode Change Start During 20-25ms," *30th International Electric Propulsion Conference*, IEPC-2007-62, Florence, Italy, 2007.

[16]Hofer, R., Johnson, L., Goebel, D., and Wirz, R., "Effects of Internally Mounted Cathodes on Hall Thruster Plume Properties," *IEEE Transactions on Plasma Science*, Vol. 36, No. 5, 2008.

[17]Sommerville, J., and King, L., "Hall-Effect Thruster Cathode Coupling Part I: Efficiency Improvements from an Extended Outer Pole," *Journal of Propulsion and Power*, Vol. 27, No. 4, 2011.

[18]Jameson, K., Goebel, D., Hofer, R., and Watkins, R., "Cathode Coupling in Hall Thrusters," *30th International Electric Propulsion Conference*, IEPC-2011-003, Florence, Italy, 2007.

[19]Farnell, C., Farnell, C., Williams, J., Williams, D., Nguyen, B., Greiner, K., and Ham, R., "Simplified Formation Process of a Low Work Function Insert," U.S. Patent 10002738, 2018.

[20]Martinez, R., Williams, J., Moritz, J. J., and Farnell, C., "Hall current plasma source having a center-mounted cathode or a surface-mounted cathode," U.S. Patent 10269526, 2019.

[21]Nakles, M., Hargus, W., Delgado, J., and Corey, R., "A Performance Comparison of Xenon and Krypton Propellant on an SPT-100 Hall Thruster," *32nd International Electric Propulsion Conference*, IEPC-2011-003, Weisbaden, Germany, 2011.

[22]Farnell, C., "Plasma Flow Field Measurements Downstream of a Hollow Cathode," Ph.D. Thesis, Colorado State University, 2007.